

1 Article

2 Investigating the Use of Pre-trained Convolutional 3 Neural Network on Cross-Subject and Cross-Dataset 4 EEG Emotion Recognition

5 Yucel Cimtay ^{1, *}, Erhan Ekmekcioglu ¹6 ¹ Institute for Digital Technologies, Loughborough University London, UK; y.cimtay@lboro.ac.uk;
7 e.ekmekcioglu@lboro.ac.uk8
9 * Correspondence: yucel.cimtay@gmail.com; y.cimtay@lboro.ac.uk

10 Received: date; Accepted: date; Published: date

11 **Abstract:** EEG has great attraction in emotion recognition studies due to its resistance to deceptive
12 actions of human. This is one of the most significant advantages of brain signals in comparison to
13 visual or speech signals in emotion recognition context. A major challenge in EEG-based emotion
14 recognition is that EEG recordings exhibit varying distributions for different people as well as for
15 the same person at different time instances. This nonstationary nature of EEG limits the accuracy of
16 it when subject independency is the priority. The aim of this study is to increase the subject-
17 independent recognition accuracy by exploiting pre-trained state of the art Convolutional Neural
18 Network (CNN) architectures. Unlike similar studies that extract spectral band power features from
19 the EEG readings, raw EEG data is used in our study after applying windowing, pre-adjustments
20 and normalization. Removing manual feature extraction from the training system overcomes the
21 risk of eliminating hidden features in the raw data and helps leverage the deep neural networks'
22 power in uncovering unknown features. To improve the classification accuracy further, median
23 filter is used to eliminate the false detections along a prediction interval of emotions. This method
24 yields mean cross-subject accuracy of 86.56% and 78.34% on SEED dataset for 2 and 3 emotion
25 classes, respectively. It also yields mean cross-subject accuracy of 72.81% on DEAP dataset and
26 81.8% on LUMED dataset for 2 emotion classes. Furthermore, the recognition model that has been
27 trained using the SEED dataset was tested with the DEAP dataset, which yields a mean prediction
28 accuracy of 58.1% across all subjects and emotion classes. Results show that in terms of classification
29 accuracy, the proposed approach is superior to, or on par with, the reference subject-independent
30 EEG emotion recognition studies identified in the literature and has limited complexity due to the
31 elimination of the need for feature extraction.

32 **Keywords:** EEG; emotion recognition; pretrained models; convolutional neural network; dense
33 layer; subject independency; dataset independency; raw data; filtering on output
34

35 1. Introduction

36 EEG is the measurement of the electrical signals which is a result of brain activities. The voltage
37 difference is measured between the actual electrode and reference electrode. There are several EEG
38 measurement devices in the market such as Neurosky, Emotiv, Neuroelectrics and Biosemi [1] which
39 provide different spatial and temporal resolutions. Spatial resolution is related to number of
40 electrodes and temporal resolution is related to the number of EEG samples processed for unit time.
41 Generally, EEG has high temporal but low spatial resolution. In terms of spatial resolution, EEG
42 electrodes can be placed on the skull according to the 10-20 or 10-10 and 10-5 positioning standards
43 [2].

44 EEG has lately been used as a powerful emotion prediction modality. It is reliable, portable and
45 relatively inexpensive compared to other brain monitoring tools and technologies. EEG has many
46 application areas. For the clinical applications, EEG is mostly used to investigate the patterns related
47 to sleep [3] and epilepsy [4]. Some other applications of EEG analysis are consciousness and
48 hyperactivity disorders [5,6], measurement of the affective components such as level of attention [7–
49 9], mental workload [10], mood and emotions [11–14] and brain computer interfaces which is the
50 work of transforming brain signals into direct instructions [15–17].

51 Human emotions have crucial effects on communication with others. Understanding the
52 emotions of human provides controlling and regulating the behaviors. As the digital world name of
53 emotion recognition, affective computing, is the work of emotion recognition by using various
54 sensors and computer-based environments. This concept was originated with Rosalind Picard's
55 paper [18] on affective computing in 1995. In EEG context, affective computing is achieved by setting
56 up brain computer interfaces (BCI) which includes sensors, machines and coding. In BCI, the
57 operation of affective computing starts with presenting users with stimuli which induces specific
58 emotions. These stimuli may be video, image, music, etc. During the session, EEG data is recorded
59 with EEG devices. The next step is typically extracting features from the recorded EEG and training
60 a classifier to predict emotion labels. The final step is testing the trained model with new EEG data
61 which is not used in training session. Data collection and labelling are the most important aspects
62 which has an impact on resulting recognition accuracy. The “Brouwer recommendations” about data
63 collection given in [19] is crucial for handling accurate data and labelling.

64 In the relevant emotion recognition literature, emotions have been broadly represented in two
65 ways. The first approach classifies emotions as discrete states such as the six basic emotions proposed
66 by Ekman and Friesen [20]. The second approach defines emotion as a continuous 4-D space of
67 valence, arousal, dominance and liking [21, 22]. In most of the studies, this space is reduced to 2-D as
68 valence and arousal dimensions [23,24]. The study conducted in [25] is very useful in the sense that
69 it relates discrete and continuous approaches to each other. Discrete emotion states are mapped on
70 to the valence-arousal circumplex model according to high number of blogposts. This study enables
71 scientists to transform emotions from continuous space to discrete space.

72 In EEG data channels, typically frequency domain analysis is used. In frequency domain the
73 most important frequency bands are delta (1-3 Hz), theta (4-7 Hz), alpha (8-13 Hz), beta (14-30 Hz)
74 and gamma (31-50 Hz) [26]. Fast Fourier Transform (FFT), Wavelet Transform (WT), eigenvector and
75 Autoregressive are the methods, which transform EEG signal from time domain to frequency domain
76 [27]. The study [28] extracts several frequency-domain features like Differential entropy (DE) and
77 energy spectrum (ES) in order to classify EEG data and [29] investigates the critical frequency bands
78 and channels for EEG based emotion recognition. One of the major problems we observed in the
79 context of emotion classification based on the analysis of EEG channels was that the classifier
80 performance fluctuates remarkably across persons as well as across dataset. Most of these approaches
81 train their classifiers using a set of features derived using the frequency domain analysis. While the
82 classifiers' performance are sufficiently high on test data, which comprise samples belonging to the
83 same subjects but excluded from training and validation, when the same classifier is applied on EEG
84 data of other subjects or on data extracted from various other datasets, the performance is degraded
85 significantly. The same problem in subject-independent analysis is not apparent in the literature in
86 the context of emotion recognition from facial expressions or other physiological data (e.g., heart rate
87 variability, electro-dermal activity). This observation has led us to investigate classification
88 approaches using raw EEG data, which preserves all information and prevents the risk of removing
89 hidden features before training the classifier.

90 2. Literature Review

91 For the classification of EEG signals, many machine learning methods such as KNN [28], SVM
92 [28–30], DT (Decision Tree) [31], Random Forest (RF) [32] and LDA (Linear Discriminant Analysis)
93 [33] are applied in this field. In deep learning context, DBN (Deep Belief Network) [34] and AE (Auto
94 encoders) [35] are studied with promising results. Besides DBN and AE, CNN and LSTM structures

95 are widely used [36–40]. Most of these models have shown good results for subject dependent
96 analysis. In [41], KNN method is employed on DEAP dataset [66] for different numbers of channels
97 which show accuracy between 82% and 88%. The study conducted in [42] quadratic time-frequency
98 distribution (QTFD) is employed to handle a high-resolution time-frequency representation of the
99 EEG and the spectral variations over time. It reports mean classification accuracies ranging between
100 73.8% and 86.2%. In [43] four different emotional states (happy, sad, angry and relaxed) are classified.
101 In that study, DWT is applied on the DEAP dataset. Wavelet features are classified using an SVM
102 classifier with Particle Swarm Optimization (PSO) [70]. The overall accuracy of 80.625% is reported
103 with valence and arousal accuracy of 86.25% and 88.125%, respectively.

104 An important issue in EEG-based emotion detection is the non-linearity and non-stationarity of
105 EEG signals. Feature sets, such as the spectral band powers of EEG channels, extracted from different
106 peoples against the same emotional states do not exhibit strong correlation. For example, galvanic
107 skin response is a robust indicator of arousal state, where different people's responses correlate with
108 each other well. Training and testing data made of EEG channels' spectral band powers and their
109 derivatives have different distributions. And it is difficult to identify sets of features from the EEG
110 recordings of different subjects, different sessions and different datasets that exhibit more
111 commonality. This makes the classification difficult with traditional classification methods, which
112 assume identical distribution. In order to address this problem and provide subject independency to
113 EEG-based emotion recognition models, deeper networks, domain adaptation and hybrid methods
114 have been applied [44,45]. Furthermore, various feature extraction techniques have been applied, and
115 different feature combinations have been tried [48,50].

116 Subject independent EEG emotion recognition, as a challenging task, has gained high interest by
117 many researchers lately. The method called Transfer Component Analysis (TCA) conducted in [44]
118 reproduces Kernel Hilbert Space, on the assumption that there exists a feature mapping between
119 source and target domain. A Subspace Alignment Auto-Encoder (SAAE) which uses non-linear
120 transformation and consistency constraint method is used in [45]. This study compares the results
121 with TCA. It achieves a leave one out mean accuracy of 77.88% in comparison with TCA, which shows
122 73.82% on SEED dataset. Moreover, mean classification accuracy for session-to-session evaluation is
123 81.81%, an improvement of up to 1.62% compared to the best baseline TCA. In one of the studies,
124 CNN with Deep domain confusion technique is applied on SEED dataset [65] and achieves 90.59%
125 and 82.16 mean accuracy for conventional (subject-dependent) EEG emotion recognition and "leave
126 one out cross validation", respectively [46]. In [47] Variational Mode Decomposition (VMD) is used
127 as a feature extraction technique and Deep Neural Network as the classifier. It gives 61.25% and
128 62.50% accuracy on DEAP dataset for arousal and valence, respectively. Another study [49] is using
129 a deep convolutional neural network with changing numbers of convolutional layers on raw EEG
130 data which is collected during music listening. It reports maximum 10-fold-validation mean accuracy
131 of 81.54% and 86.87% for arousal and valence, respectively. It also achieves 56.22% of arousal and
132 68.75% of valence accuracies for one-subject-out test. As can be seen, the reported mean accuracy
133 levels drop considerable in one-subject-out tests due to the nature of the EEG signals.

134 The study [50] extracts totally 10 different linear and nonlinear features from EEG signals. The
135 linear features are Hjorth activity, Hjorth mobility, Hjorth complexity, the standard deviation, PSD-
136 Alpha, PSD Beta, PSD-Gamma, PSD-Theta and the nonlinear features are sample entropy and
137 wavelet entropy. By using a method called Significance Test/sequential Backward Selection and the
138 Support Vector Machine (ST-SBSSVM) which is a combination of the significance test, sequential
139 backward selection, and support vector machine, it achieves 72% cross subject accuracy for DEAP
140 dataset with High-Low valence classification. It also achieves 89% maximum cross subject accuracy
141 for SEED dataset with positive-negative emotions. Another study [51] uses FAWT (Flexible Analytic
142 Wavelet Transform) which decomposes EEG signals into sub bands. Random forest and SVM are
143 used for classification. The mean classification accuracies are 90.48% for positive/neutral/negative
144 (three classes) in the SEED dataset; 79.95% for high arousal (HA)/low arousal (LA) (two classes);
145 79.99% for the high valence (HV)/low valence (LV) (two classes); and 71.43% for
146 HVHA/HVLA/LVLA/LVHA (four classes) in the DEAP dataset. In [52] transfer recursive feature

147 elimination (T-RFE) technique is used to determine a set of the most robust EEG features for stable
148 distribution across subjects. This method is validated on DEAP dataset, the classification accuracy
149 and F-score for arousal is 0.7867, 0.7526 and 0.7875, 0.8077 for valence. A regularized graph neural
150 network (RGNN) is applied in [53] for EEG-based emotion recognition, which includes inter-channel
151 relations. The classification accuracy results on SEED dataset are 64.88%, 60.69%, 60.84%, 74.96%,
152 77.50%, 85.30% for delta, theta, alpha, beta, gamma and all bands. Moreover, it achieves 73.84% of
153 accuracy on SEED IV [71] dataset.

154 There are several studies which apply transfer learning which aims to explore common stable
155 features and apply to other subjects [54]. In terms of affective computing, the work is exploring some
156 common and stable features which are invariant between subjects. This is also called domain
157 adaptation. In [55] the scientists tried to find typical spatial pattern filters from various recording
158 sessions and have applied these filters on the following ongoing EEG samples. Subject dependent
159 spatial and temporal filters are derived from 45 subjects and a representative subset is chosen in [56].
160 The study [57] uses compound common spatial patterns which are the sum of covariance matrices.
161 The aim of this technique is to utilize the common information which is shared between different
162 subjects. The other important studies which apply different domain adaptation techniques on SEED
163 dataset are [58–61]. The common properties of these domain adaptation techniques are exploring an
164 invariant feature subspace which reduces the inconsistencies of EEG data between subjects or
165 different sessions. In the study in [62] domain adaptation technique is applied not only in cross-
166 subject context but also for cross datasets. The trained model in SEED dataset is tested against DEAP
167 dataset and vice versa. It reports an accuracy improvement of 7.25%-13.40% with domain adaptation
168 compared to the one without domain adaptation. Scientists applied an adaptive subspace feature
169 matching (ASFM) in [63] in order to integrate both the marginal and conditional distributions within
170 a unified framework. This method achieves 83.51%, 76.68%, 81.20% classification accuracies for the
171 first, second and third sessions of SEED dataset, respectively. This study also conduct testing between
172 sessions. For instance, it trains the model with the data of first session and test on the second session
173 data. In domain adaptation method, the conversion of features into a common subspace may lead to
174 data loss. In order to avoid this, a Deep Domain Confusion (DDC) method based on CNN architecture
175 is used [64]. This study uses adaptive layer and domain confusion loss based on Maximum Mean
176 Discrepancy (MMD) to automatically learn a representation jointly trained to optimize classification
177 and domain invariance. The advantage of this is adaptive classification with retaining the original
178 distribution information.

179 Having observed that the distribution of commonly derived sets of features from EEG signals
180 show differences between subjects, sessions and datasets, we anticipate that there could be some
181 invariant feature sets that follow common trajectories across subjects, sessions and datasets. There is
182 a lack of studies that investigate these additional feature sets in the EEG signals that can contribute
183 to robust emotion recognition across subjects. The aim of this study is to uncover these kinds of
184 features in order to achieve promising cross-subject EEG-based emotion classification accuracy with
185 manageable processing loads. For this purpose, raw EEG channel recordings after normalization and
186 a state-of-the-art pre-trained CNN model are used. The main motivation behind choosing a pre-
187 trained CNN architecture is due to their superiority in feature extraction and inherent exploitation of
188 domain adaptation. To improve the emotion recognition accuracy, additionally in the test phase, a
189 median filter is used in order to reduce the evident false alarms.

190 2.1 Contributions of the Work

191 The contributions of this work to the related literature in EEG-based emotion recognition can be
192 summarized as follows:

- 193 • Feature extraction process is completely left to a pretrained state-of-the-art CNN model
194 InceptionResnetV2 whose capability of feature extraction is shown as highly competent in
195 various classification tasks. This enables the model to explore useful and hidden features for
196 classification.

- 197 • Data normalization is applied in order to remove the effects of fluctuations in the voltage
198 amplitude and protect the proposed network against probable ill-conditioned situations.
- 199 • Extra pooling and dense layers are added to the pretrained CNN model in order to increase
200 its depth, so that the classification capability is enhanced.
- 201 • The output of the network is post-filtered in order to remove the false alarms, which may
202 emerge in short intervals of time where the emotions are assumed to remain mostly
203 unchanged.

204 3. Materials

205 The EEG datasets used in this work are SEED [65], the EEG data of DEAP [66] and our own EEG
206 dataset [76] which is a part of multimodal emotional database LUMED (Loughborough University
207 Multimodal Emotion Database). All the datasets are open to public access.

208 3.1 Overview of the SEED Dataset

209 SEED dataset is a collection of EEG recordings which is prepared by BCMI laboratory of
210 Shanghai Jiao Tong University. 15 clips are chosen for eliciting (neutral, negative and positive)
211 emotions. Each stimuli session is composed of 5 sec. of hint of movie, 4 min. of clip, 45 sec. of self-
212 assessment and 15 sec. of rest. There are 15 Chinese subjects (7 females and 8 males) participated in
213 this study. Each participant had 3 sessions on different days. Totally 45 session of EEG data has been
214 recorded. The labels are given according to the clip contents (-1 for negative, 0 for neutral and 1 for
215 positive). The data was collected via 62 channels which are placed according to 10-20 system, down
216 sampled to 200Hz, a bandpass frequency filter from 0-75Hz was applied and presented as MATLAB
217 "mat" files.

218 3.2 Overview of the DEAP Dataset

219 DEAP [22] is a multimodal dataset which includes the electroencephalogram (EEG) and
220 peripheral physiological signals of 32 participants. For 22 of the 32 participants, frontal face video
221 was also recorded. Data was recorded while one-minute long music videos were watched by
222 participants. Totally 40 videos were shown to each participant. The videos were rated by the
223 participants in terms of levels of arousal, valence, like/dislike, dominance and familiarity which
224 changes between 1 and 9. EEG data is collected with 32 electrodes. The data was down sampled to
225 128Hz, EOG artefacts were removed, a bandpass frequency filter from 4.0-45.0Hz was applied. The
226 data was segmented into 60 second intervals and a 3 second baseline data was removed.

227 3.3 Overview of the LUMED Dataset

228 LUMED (Loughborough University Multimodal Emotion Dataset) is a new multimodal dataset
229 that was created in Loughborough University London (UK), by collecting simultaneous multimodal
230 data from 11 participants (4 females and 7 males). The modalities include visual data (face RGB),
231 peripheral physiological signals (galvanic skin response, heartbeat, temperature) and EEG. These
232 data were collected from participants while they were presented with audio-visual stimuli loaded
233 with different emotional content. Each data collection session lasted approximately 16 minutes long
234 that consists of short video clips playing one after the other. The longest clip was approximately 2.5
235 minutes and the shortest one was 1 minute long. Between each clip, in order to provide the participant
236 a refresh and rest, a 20 second-long gray screen was displayed. Although the emotional ground truth
237 of each clip was estimated based on the content, in reality, a range of different emotions might be
238 triggered for different participants. For this purpose, after each session, the participants were asked
239 to label the clips they watched with the most dominant emotional state they felt. In this current study,
240 we exploited the EEG modality of the LUMED dataset only. For this study, we have re-labelled the
241 samples, such that only 2 classes were defined as negative valence and positive valence. This is done
242 to make a fair comparison with other studies. Moreover, each channel's data was filtered in the
243 frequency range of 0.5Hz to 75Hz to attenuate the high frequency components that are not believed

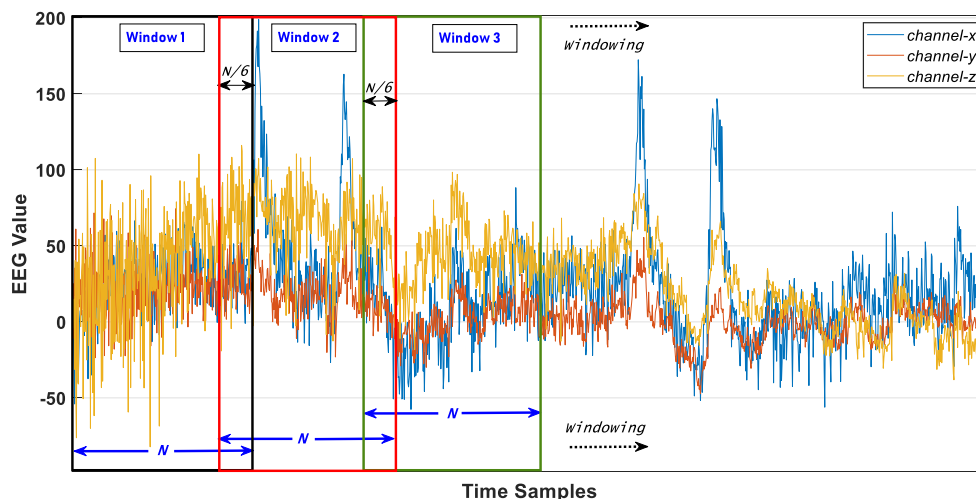
244 to be have a meaningful correlation with the emotion classes. Normally, captured EEG signals are
 245 noisy with EMG (electromyogram) and EOG (electrooculogram) type artefacts. EMG artefacts are
 246 electrical noise resulted from facial muscle activities and EOG is electrical noise due to eye
 247 movements. For traditional classification and data analysis methods, in order to prevent heavily
 248 skewed results, these kinds of artefacts should be removed from the EEG channel data through
 249 several filtering stages. As an example, the study in [87] removes the eye movement artefacts from
 250 signal by applying ICA (Independent Component Analysis). LUMED dataset has been created
 251 initially with the purpose of training a deep-learning based emotion recognition system, described in
 252 Section 4. Depending on the type and purpose of other supervised machine learning systems, this
 253 dataset could require a more thorough pre-processing for artefact removal. In LUMED, EEG data was
 254 captured based on 10-20 system by Neuroelectronics Enobio 8 [82], an 8-channel EEG device with a
 255 temporal resolution of 500 Hz. The used channels were FP1, AF4, FZ, T7, C4, T8, P3, OZ, which are
 256 spread over frontal, temporal and center lobes of the brain.

257 4. Proposed Method

258 In this work, the emotion recognition model works on raw EEG signals without pre-feature
 259 extraction. Feature extraction is left to a state-of-the-art CNN model: InceptionResnetV2. The success
 260 of this pretrained CNN model on raw data classification was extensively outlined in [67]. Since the
 261 distribution of EEG data shows variations from person to person, session to session, and dataset to
 262 dataset, it is difficult to identify a feature set that exhibits good accuracy every time. On the other
 263 hand, pretrained CNN models are very competent in feature extraction. Therefore, this work gets use
 264 of it.

265 4.1 Windowing of Data

266 Data is split into fixed length (N) windows with an overlapping size of $N/6$ as shown in Figure
 267 1 (displayed for 3 random channels). One window of EEG data is given in Figure 2 where M is the
 268 number of selected channels, C_{ab} is " b^{th} data point of channel a ".
 269



270

271

Figure 1 Windowing with overlapping on raw EEG data

272 4.2 Data Reshaping

273

274 EEG data is reshaped to fit the input layer properties of InceptionResnetV2 which is shown in
 275 Figure 2. KERAS, which is an open-source neural network library written in Python, is used for the
 276 training purpose. Since KERAS is used for training purpose, the minimum input size should be $(N_1, N,$
 277 $3)$ for InceptionResnetV2 where $N_1 \geq 75$, $N \geq 75$ [68]. Depending on the number of selected
 278 channels, each channel data is augmented by creating the noisy copies of it. For instance, if the

279 number of selected channels is S , for each channel the number of noisy copies is calculated according
 280 to Equation 1 where $ceil$ operator rounds the number to the next integer (if the number is not
 281 integer) and NNC is number of noisy copies.

282

$$NNC = ceil\left(\frac{N_1}{S}\right) - 1, \quad (1)$$

283

284 The noisy copies of each channel are created by adding random samples of a gaussian
 285 distribution of mean μ and variance σ^2 where μ and σ are chosen as 0 and 0.01, respectively. This
 286 process is given in Equation 2 where $[\tilde{C}_{a1}, \tilde{C}_{a2}, \dots, \tilde{C}_{aN}]$ is the noisy copy of the original data
 287 $[C_{a1}, C_{a2}, \dots, C_{aN}]$ and $[n_{a1}, n_{a2}, \dots, n_{aN}]$ is the noise vector.

288

$$[\tilde{C}_{a1}, \tilde{C}_{a2}, \dots, \tilde{C}_{aN}] = [C_{a1}, C_{a2}, \dots, C_{aN}] + [n_{a1}, n_{a2}, \dots, n_{aN}], \quad (2)$$

289

290 Since the samples are randomly chosen, each noisy copy is different from each other. N is
 291 related to the windowing size. Therefore, a window size N greater than or equal to 75 is chosen.
 292 We chose N as 300 in order to provide a standard window size for datasets. This corresponds to 1.5
 293 secs for SEED dataset, approximately 2 secs for DEAP dataset and 0.6 sec for LUMED dataset.
 294 Moreover, we chose N_1 as 80 for all datasets. Augmentation process is repeated 3 times in order to
 295 make the data to fit KERAS input size. This work does not use interpolation between channels due
 296 to that EEG is a nonlinear signal. The reason for adding noise is mainly for data augmentation. There
 297 are several ways of data augmentation such as rotation, shifting and adding noise. In the image
 298 processing context, rotation, shifting, zooming and adding noise are used. However, we only use
 299 noise addition for EEG data augmentation in order to both keep the channel's original data and create
 300 new augmented data with limited gaussian noise. This is as if there was another electrode very close
 301 the electrode, which is augmented with additional noise. We use data augmentation instead of data
 302 duplication in order to make the network adapt to the noisy data and increase the prediction
 303 capability of it. This also prevents the network from overfitting due to data repetition. This technique
 304 was similarly applied in [83].

305

306 4.3 Normalization

307

308 Following windowing, augmentation and reshaping, each channel data is normalized by
 309 removing mean of each window from each sample. This is repeated for all channels and the noisy
 310 copies. The aim of removing the mean is to equate the mean value of each window to 0. This protects
 311 the proposed network against probable ill-conditioned situations. In MATLAB, this process is
 312 applied automatically on the input data. In KERAS, we performed this manually just before training
 313 the network. Each dimension is created separately so they are different from each other.

314

315

316

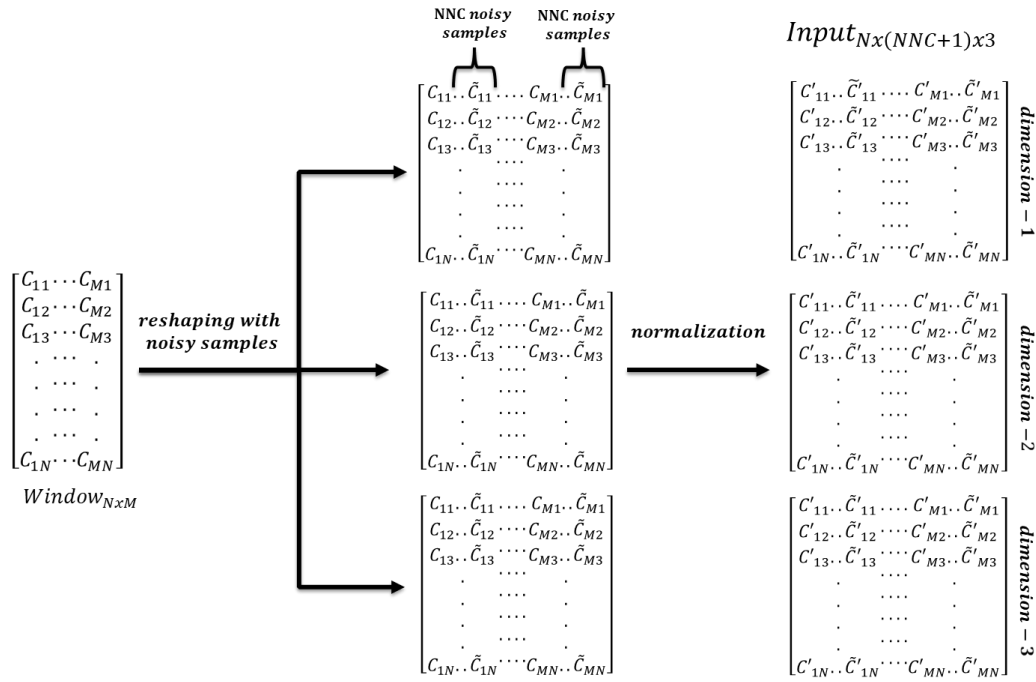


Figure 2 Windowing, Reshaping and Normalization on EEG data

317

318

319 4.4 Channel Selection

320

321

322

323

324

325

326

327

328

329

330

331

332

333

334

335

336

337

338

339

340

341

342

343

344

In this work, we concentrated on the frontal temporal lobes of the brain. As it is stated in [72,73], emotion changes mostly affect the EEG signals on the frontal and temporal lobes. Different number of channels are tried in this work and increasing the number of channels does not help improve the accuracy. Because, technically, including the channels in the model, which are not correlated with the emotion changes, does not help and on the contrary can adversely affect the accuracy. It is also known that the electrical relations between asymmetrical channels are determining the arousal and valence, hence the emotion [74,75]. Therefore, we have chosen 4 asymmetrical pairs of electrodes: AF1, F3, F4, F7, T7, AF2, F5, F8 and T8 from frontal and temporal lobes which are equally spread on the skull. The arrangement of these channels in the window is AF1, AF2, F3, F4, F5, F6, F7, T7, T8.

331 4.5 Network Structure

In this work a pretrained CNN network, InceptionResnetV2, is used as base model. Following InceptionResnetV2, Global Average Pooling layer is added for decreasing the data dimension and extra dense layers (fully connected layers) are added in order to increase the depth and success for classifying complex data. The overall network structure is given in Figure 3, and the properties of the layers following the CNN is described in Table 1. The training parameters are specified in Table 2. In Figure 3, Dense Layer-5 determines the number of output classes and *argMax* selects the one with the maximum probability. We use “relu” activation function to cover the interaction effects and non-linearities. This is very important in our problem while using a deep learning model. Relu is one of the most widely used and successful activation functions in the field of artificial neural networks. Moreover, at the last dense layer we use the “softmax” activation in order to produce the class probabilities.

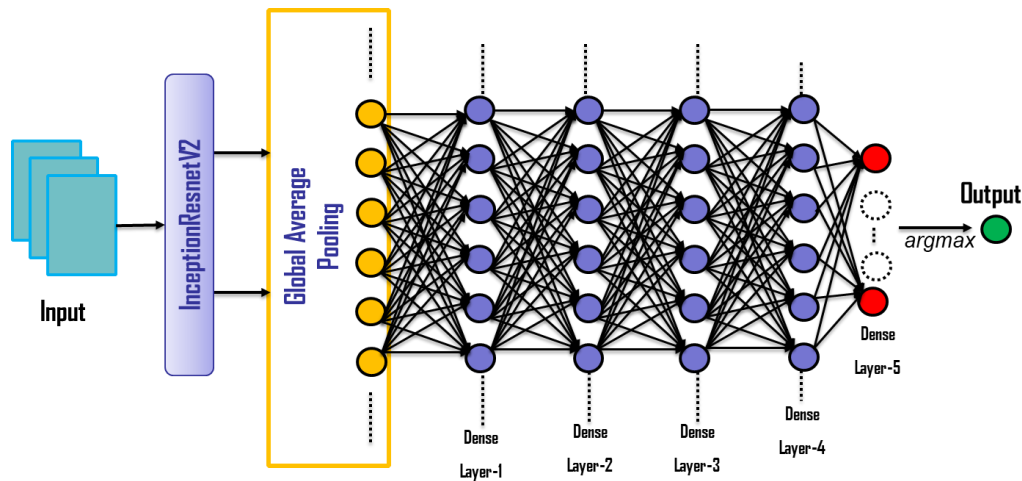


Figure 3 The structure of proposed network model.

Table 1. The properties of Layers following InceptionResNetV2 base model.

| Layer (Type) | Output shape | Connected to | Activation Function |
|------------------------|----------------|------------------------|---------------------|
| Global_Average_Pooling | (None, 1536) | convolution | - |
| Dense 1 | (None, 1024) | Global_Average_Pooling | Relu |
| Dense 2 | (None, 1024) | Dense 1 | Relu |
| Dense 3 | (None, 1024) | Dense 2 | Relu |
| Dense 4 | (None, 512) | Dense 3 | Relu |
| Dense 5 | (None, z^1) | Dense 4 | Softmax |

¹ z is set according to the number of output classes.

Table 2. The training parameters of network.

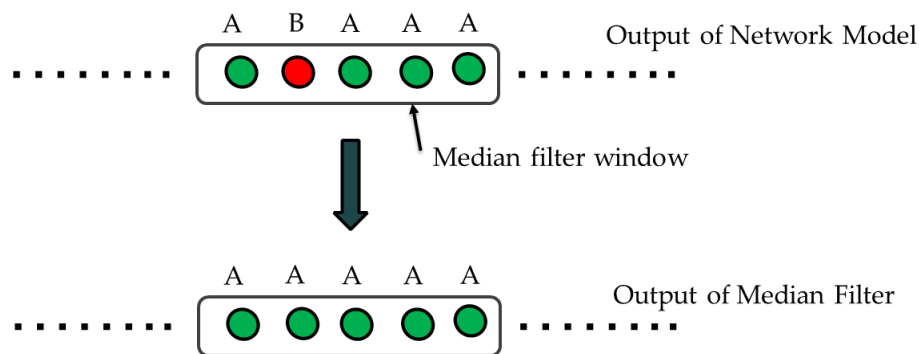
| Property | Value |
|-------------------|--|
| Base model | InceptionResNetV2 |
| Additional layers | Global Average Pooling, 5 Dense Layers |
| Regularization | L2 |
| Optimizer | Adam |
| Loss | Categorical cross entropy |
| Max. # Epochs | 100 |
| Shuffle | True |
| Batch size | 64 |
| Environment | Win 10, 2 Parallel GPU(s), TensorFlow |
| # Output classes | 2 (Pos-Neg) or 3 (Pos-Neu-Neg) |

4.6 Filtering on Output Classes

Since EEG is very prone to noise and different type of artifacts, filtering of EEG signals is widely studied in EEG recognition context. The study conducted in [84] compares three types of smoothing filters (smooth filter, median filter and Savitzky–Golay) on EEG data for the medical diagnostic purposes. The authors concluded that the most useful filter is the classical Savitzky–Golay since it smooths the data without distorting the shape of the waves.

359 Another EEG data filtering study is provided in [85]. This study employs a moving average
 360 filtering on extracted features and then classifies the signal by using SVM (Support Vector Machine).
 361 It achieves very promising accuracy results with limited processing time compared to similar studies.

362 Emotions change quicker than moods for healthy people [69]. However, in very short time
 363 intervals (in the range of few seconds), the emotions show lesser variance in healthy individuals with
 364 good emotion regulation. Different from the studies [84, 85], the filtering is applied on the output in
 365 our method. It is assumed that in a defined small-time interval T the emotion state does not change.
 366 Therefore, we apply a median filter on the output data inside a specific time interval with an aim of
 367 removing the false alarms and increase the overall emotion classification accuracy. This process is
 368 shown in Figure 4 where A and B stands for different classes.
 369

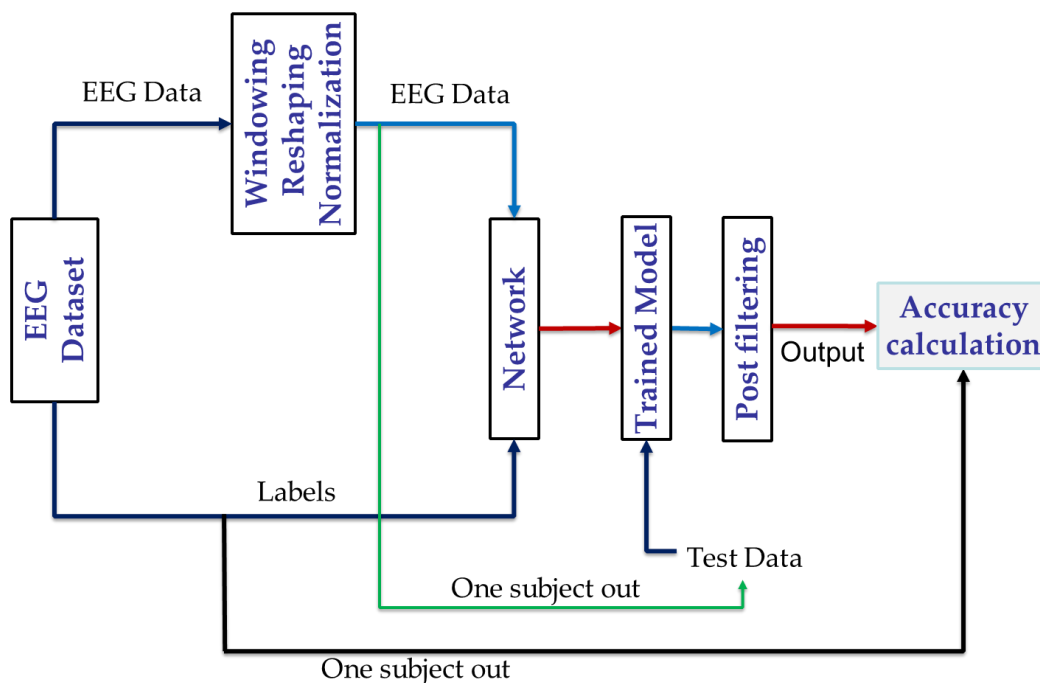


370

371

Figure 4 Filtering on Output

372 The overall process that describes how model training and testing is carried out is visually depicted
 373 in Figure 5.



374

375 Figure 5 Overall training and testing process of the EEG-based emotion recognition model

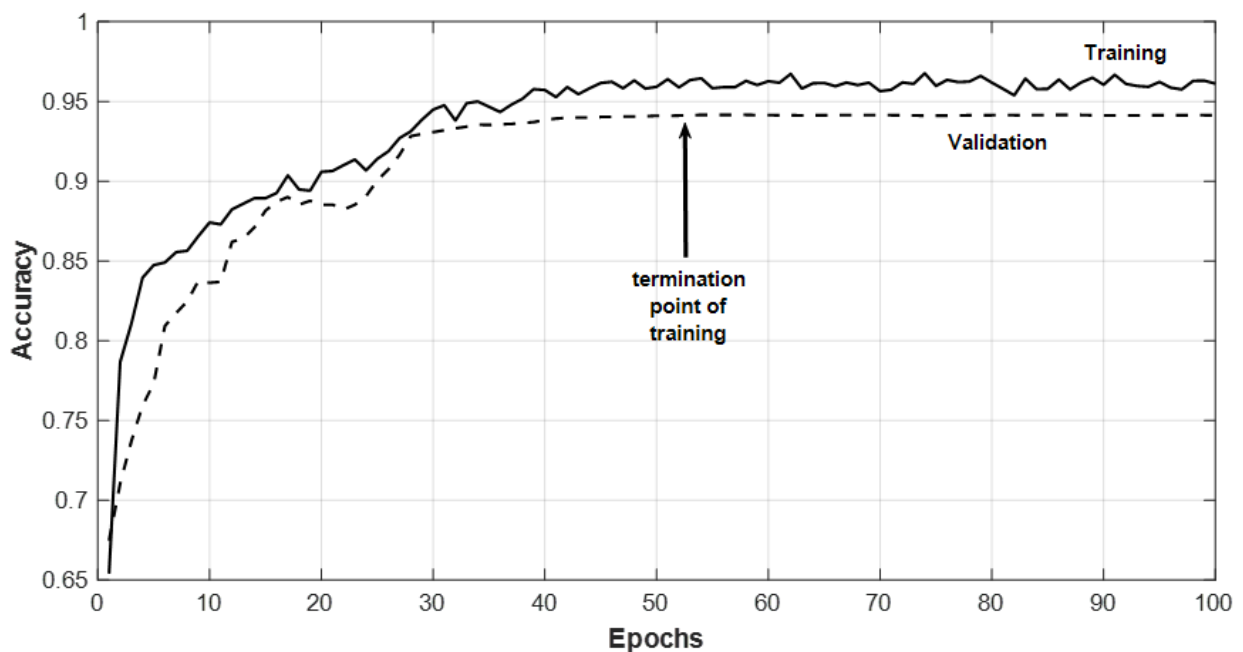
376 5. Results and Discussions

377 In this work, for SEED dataset, classification tests are conducted for 2 categories of classification:
 378 2-classes: Positive-Negative valence (Pos-Neg) and 3-classes: Positive-Neutral-Negative valence (Pos-

379 Neu-Neg). SEED dataset provides the labels as negative, neutral and positive. DEAP dataset labels
 380 the valence and arousal between 1 and 9. The valence values above 4.5 are taken as positive and the
 381 values smaller than 4.5 are taken as negative. For LUMED dataset, classification is done as either
 382 positive or negative valence. One-subject-out classification for each dataset are conducted and the
 383 results are compared to several reference studies, which provide cross-subject and cross-dataset
 384 results. In one-subject-out tests, one subject's data is excluded completely from the training set. The
 385 remaining training set is divided into training and validation sets. In this work, during training, when
 386 we do not see improvement on validation accuracy for 6 consecutive epochs, we stopped the training
 387 and applied the test data on the final model. An example is shown in Figure 6. For each user, Table 3
 388 depicts one-subject-out tests for SEED dataset based on all sessions together, with and without
 389 normalization and with and without output filtering. We also got the accuracy results without
 390 pooling and dense layers. The mean accuracies dropped by 8.3% and 11.1% without pooling and
 391 dense layers, respectively. Applying median filter on the predicted output improves the mean
 392 accuracy by approximately 4% for SEED dataset. The filter size is empirically and set to 5. This
 393 corresponds approximately to 6 seconds of data. In this time interval it is assumed that the emotion
 394 state remains unchanged. It can be seen in Table 3 that the accuracy for some users is high and for
 395 some users it is relatively lower. This is based on the modeling of the network with the remaining
 396 training data after excluding the test data. However standard deviation is still acceptable. Another
 397 issue is that when the number of classes is increased from 2 (Pos-Neg) to 3 (Pos-Neg-Neu), the
 398 prediction accuracies drop. This is because some samples labelled as neutral might fall into the
 399 negative or the positive classes.

400 One of the most important characteristics of our work in this paper is that we provide the
 401 accuracy scores for each subject separately. This is not observed in most of the other reference studies
 402 that tackle EEG-based emotion recognition.

403
 404



405
 406

Figure 6 An example of network training

407

408

Table 3. "One subject out" classification accuracies for SEED dataset.

| Users | Accuracy (Pos-Neg) ¹ | Accuracy (without normalization) | Accuracy (with filtering) | Accuracy (Pos-Neu-Neg) ² | Accuracy (without normalization) | Accuracy (with filtering) |
|-------|---------------------------------|----------------------------------|---------------------------|-------------------------------------|----------------------------------|---------------------------|
|-------|---------------------------------|----------------------------------|---------------------------|-------------------------------------|----------------------------------|---------------------------|

| | | (Pos-Neg) | (Pos-Neg) | | (Pos-Neu-Neg) | (Pos-Neu-Neg) |
|----------|-------|-----------|-----------|------|---------------|---------------|
| User 1 | 85.7 | 74.2 | 88.5 | 73.3 | 55.2 | 78.2 |
| User 2 | 83.6 | 76.3 | 86.7 | 72.8 | 57.4 | 78.5 |
| User 3 | 69.2 | 56.7 | 74.3 | 61.6 | 53.9 | 67.7 |
| User 4 | 95.9 | 69.4 | 96.1 | 83.4 | 72.4 | 88.3 |
| User 5 | 78.4 | 70.1 | 83.2 | 74.1 | 54.3 | 76.5 |
| User 6 | 95.8 | 81.8 | 96.4 | 85.3 | 67.7 | 89.1 |
| User 7 | 72.9 | 56.2 | 77.7 | 64.4 | 53.5 | 70.3 |
| User 8 | 69.2 | 49.3 | 75.2 | 62.9 | 51.3 | 69.2 |
| User 9 | 88.6 | 61.5 | 90.5 | 79.2 | 64.8 | 82.7 |
| User 10 | 77.8 | 70.1 | 82.7 | 69.3 | 56.0 | 74.5 |
| User 11 | 78.6 | 65.7 | 83.1 | 73.0 | 59.9 | 78.1 |
| User 12 | 81.6 | 72.0 | 85.7 | 75.6 | 63.2 | 78.4 |
| User 13 | 91.2 | 80.2 | 94.2 | 81.3 | 73.1 | 84.9 |
| User 14 | 86.4 | 72.3 | 91.8 | 73.9 | 61.1 | 78.5 |
| User 15 | 89.2 | 73.9 | 92.3 | 75.4 | 60.3 | 80.3 |
| Average | 82.94 | 68.64 | 86.56 | 73.7 | 60.27 | 78.34 |
| Std.Dev. | 8.32 | 8.88 | 6.94 | 6.80 | 6.59 | 6.11 |

409 ¹ Pos-Neg: Positive-Negative, ² Pos-Neu-Neg: Positive-Neutral-Negative.

410

411

412 Table 4 shows the cross-subject accuracy comparison of several top studies, which provides the
 413 results for 2-classes (Pos-Neg) or 3-classes (Pos-Neu-Neg). For Pos-Neg, the proposed method
 414 achieves 86.5% accuracy which is slightly lower than ST-SBSSVM [50]. However, our method has far
 415 less complexity, since it does not depend on pre-feature extraction and associated complex
 416 calculations. Furthermore, it is not clear in [50] if the reported maximum accuracy of ST-SBSSVM
 417 corresponds to the mean prediction accuracy of all subjects, or the maximum prediction accuracy of
 418 any subject amongst all.

418

419

420

421

422

423

424

425

426

427

428

429

430

431

432

Table 4. “One-subject-out” prediction accuracies of reference studies using the SEED dataset.

| Work | Accuracy (Pos-Neg) | Accuracy (Pos-Nue-Neg) |
|-----------------|-----------------------|---------------------------|
| ST-SBSSVM [50] | 89.0 | - |
| RGNN [53] | - | 85.3 |
| Proposed | 86.5 | 78.3 |
| CNN-DDC [46] | - | 82.1 |
| ASFM [63] | - | 80.4 |
| SAAE [45] | - | 77.8 |
| TCA [44] | - | 71.6 |

| | |
|-----------|------|
| GFK [77] | 67.5 |
| KPCA [78] | 62.4 |
| MIDA [79] | 72.4 |

433

434

435

436

437

438

439

440

441

442

443

Table 5 shows the accuracy results of proposed model for DEAP database for 2-classes (Pos-Neg). Generally, the reported accuracies are lower than the ones achieved in the SEED dataset. This may be due to poorer labelling quality of the samples in the DEAP dataset. Some reference studies employ varying re-labelling strategies on the samples of the DEAP dataset to revise class labels. This automatically increases the reported prediction accuracy levels. However, we decided not to alter and respect the original labelling strategy used in that dataset. We only set the threshold in the exact midpoint of the scale of 1 to 9 to divide the samples into two classes, positive and negative. It is acceptable to achieve slightly lower accuracy values than some others as shown in Table 6. To reiterate, post median filtering improves the mean prediction accuracy by approximately 4%.

444

Table 5. “One-subject-out” prediction accuracies for DEAP dataset using 2-classes (Pos-Neg)

| Users | Accuracy | Accuracy (with median filtering) |
|----------------|--------------|--|
| User 1 | 65.1 | 69.2 |
| User 2 | 71.2 | 73.4 |
| User 3 | 67.8 | 69.1 |
| User 4 | 61.7 | 65.3 |
| User 5 | 73.1 | 75.9 |
| User 6 | 82.5 | 85.4 |
| User 7 | 75.5 | 77.2 |
| User 8 | 67.6 | 71.3 |
| User 9 | 62.8 | 67.9 |
| User 10 | 61.9 | 66.6 |
| User 11 | 68.8 | 72.5 |
| User 12 | 64.3 | 69.8 |
| User 13 | 69.1 | 74.9 |
| User 14 | 64.3 | 68.8 |
| User 15 | 65.6 | 70.2 |
| User 16 | 68.7 | 72.1 |
| User 17 | 65.6 | 70.7 |
| User 18 | 75.8 | 78.3 |
| User 19 | 66.9 | 72.1 |
| User 20 | 70.4 | 73.2 |
| User 21 | 64.5 | 68.8 |
| User 22 | 61.6 | 68.3 |
| User 23 | 80.7 | 83.6 |
| User 24 | 62.5 | 69.4 |
| User 25 | 64.9 | 70.1 |
| User 26 | 69.7 | 72.9 |
| User 27 | 82.7 | 85.3 |
| User 28 | 68.9 | 73.8 |
| User 29 | 61.7 | 69.9 |
| User 30 | 72.9 | 77.7 |
| User 31 | 73.1 | 78.4 |
| User 32 | 63.6 | 68.1 |
| Average | 68.60 | 72.81 |

| | | |
|------------------|------|------|
| Std. Dev. | 5.85 | 5.07 |
|------------------|------|------|

445
446
447
448
449
450
451
452
453
454

Table 6 shows the prediction accuracies of several studies that use the DEAP dataset for 2 classes (Pos-Neg). Our proposed method yields promising accuracy results with only limited complexity (e.g., without any pre-feature extraction cycle) when compared to others. For all eight incoming EEG data channels, the windowing, reshaping, normalization and classification processes take on average 0.34 sec on the test workstation (Core i-9, 3.6 GHz, 64 Gb RAM). This is the computational time used by the python script and KERAS framework. Hence, the data classification can be achieved with roughly a delay of half a second, rendering our usable in real time systems.

455

Table 6. One-subject-out accuracy comparison of several studies for DEAP dataset (Pos-Neg).

| Work | Accuracy |
|-----------------|-----------------|
| FAWT [51] | 79.9 |
| T-RFE [52] | 78.7 |
| Proposed | 72.8 |
| ST-SBSSVM [50] | 72 |
| VMD-DNN [47] | 62.5 |
| MIDA [79] | 48.9 |
| TCA [44] | 47.2 |
| SA [80] | 38.7 |
| ITL [81] | 40.5 |
| GFK [77] | 46.5 |
| KPCA [78] | 39.8 |

456
457
458
459

Table 7 shows the accuracy results of our proposed model on the LUMED dataset for 2-classes (Pos-Neg). It produces a mean prediction accuracy of %81.8 with a standard deviation of 10.9. Post media filtering increases the mean accuracy by approximately 4.5%.

460

Table 7. One-subject-out prediction accuracies for the LUMED dataset.

| | Accuracy | Accuracy (with filtering) |
|------------------|-----------------|--------------------------------------|
| User 1 | 85.8 | 87.1 |
| User 2 | 56.3 | 62.7 |
| User 3 | 82.2 | 86.4 |
| User 4 | 73.8 | 78.5 |
| User 5 | 92.1 | 95.3 |
| User 6 | 67.8 | 74.1 |
| User 7 | 66.3 | 71.4 |
| User 8 | 89.7 | 93.5 |
| User 9 | 86.3 | 89.9 |
| User 10 | 89.1 | 93.4 |
| User 11 | 58.9 | 67.6 |
| Average | 77.11 | 81.80 |
| Std. Dev. | 12.40 | 10.92 |

461
462
463
464

In this work, cross-dataset tests are also conducted between the SEED-DEAP, SEED-LUMED and DEAP-LUMED datasets for positive and negative labels. Table 8 shows the cross-dataset accuracy results between SEED and DEAP. Our model is trained using the data in the SEED dataset and tested on the DEAP dataset separately. It yields 58.10% mean prediction

465 accuracy that is promising in this context. The comparison of the cross-dataset performance of
 466 our proposed model with the other cross-dataset studies is given in Table 9. The cross-dataset
 467 accuracy of our model is consistently superior to other studies. Table 10 shows the cross-dataset
 468 results between SEED-LUMED and DEAP-LUMED. Since LUMED is a new dataset we cannot
 469 give any benchmark results with other studies. However, the mean accuracy results and
 470 standard deviations are promising.

471 **Table 8.** Cross-dataset prediction accuracy results (Trained on SEED and Tested on DEAP)

| Users | Accuracy (Pos-Neg) | Accuracy (with median filtering) (Pos-Neg) |
|------------------|-----------------------|--|
| User 1 | 50.5 | 54.9 |
| User 2 | 61.7 | 63.7 |
| User 3 | 43.3 | 47.3 |
| User 4 | 46.0 | 51.5 |
| User 5 | 68.9 | 71.9 |
| User 6 | 45.3 | 49.4 |
| User 7 | 73.4 | 77.2 |
| User 8 | 51.9 | 56.3 |
| User 9 | 62.3 | 67.9 |
| User 10 | 63.8 | 68.6 |
| User 11 | 48.6 | 53.6 |
| User 12 | 46.4 | 51.3 |
| User 13 | 50.1 | 57.1 |
| User 14 | 70.4 | 76.9 |
| User 15 | 58.8 | 62.8 |
| User 16 | 59.7 | 66.3 |
| User 17 | 46.6 | 53.1 |
| User 18 | 64.7 | 68.5 |
| User 19 | 47.9 | 53.3 |
| User 20 | 39.1 | 44.6 |
| User 21 | 62.1 | 68.8 |
| User 22 | 45.6 | 51.3 |
| User 23 | 61.4 | 69.9 |
| User 24 | 54.0 | 59.2 |
| User 25 | 50.8 | 56.3 |
| User 26 | 40.8 | 44.7 |
| User 27 | 39.2 | 45.3 |
| User 28 | 42.4 | 48.4 |
| User 29 | 46.2 | 50.3 |
| User 30 | 41.7 | 46.2 |
| User 31 | 61.4 | 65.7 |
| User 32 | 53.8 | 57.1 |
| Average | 53.08 | 58.10 |
| Std. Dev. | 9.54 | 9.51 |

472

473 **Table 9.** One-subject-out cross-dataset prediction accuracy and standard deviation comparison of
 474 several studies (Trained on SEED and Tested on DEAP)

| Work | Accuracy (Pos-Neg) | Standard Deviation |
|------|--------------------|--------------------|
|------|--------------------|--------------------|

| | | |
|-----------------|--------------|-------------|
| Proposed | 58.10 | 9.51 |
| MIDA [79] | 47.1 | 10.60 |
| TCA [44] | 42.6 | 14.69 |
| SA [80] | 37.3 | 7.90 |
| ITL [81] | 34.5 | 13.17 |
| GFK [77] | 41.9 | 11.33 |
| KPCA [78] | 35.6 | 6.97 |

475 **Table 10.** Cross-dataset prediction accuracy results (Trained on SEED/DEAP and Tested on LUMED)

| Users (LUMED) | Trained on SEED | | Trained on DEAP | |
|------------------|-----------------------|--|-----------------------|--|
| | Accuracy (Pos-Neg) | Accuracy (with median filtering) (Pos-Neg) | Accuracy (Pos-Neg) | Accuracy (with median filtering) (Pos-Neg) |
| User 1 | 68.2 | 72.3 | 42.7 | 48.3 |
| User 2 | 54.5 | 61.7 | 50.4 | 56.8 |
| User 3 | 54.3 | 59.6 | 49.7 | 54.1 |
| User 4 | 59.6 | 64.1 | 51.3 | 57.9 |
| User 5 | 44.8 | 53.7 | 87.1 | 89.7 |
| User 6 | 67.1 | 73.5 | 52.6 | 58.4 |
| User 7 | 53.2 | 60.8 | 53.8 | 59.2 |
| User 8 | 64.5 | 71.2 | 46.0 | 49.3 |
| User 9 | 48.6 | 50.9 | 84.7 | 85.6 |
| User 10 | 64.9 | 76.3 | 51.5 | 58.8 |
| User 11 | 57.1 | 64.8 | 63.8 | 67.1 |
| Average | 57.89 | 64.44 | 57.6 | 62.29 |
| Std. Dev. | 7.33 | 7.82 | 14.23 | 12.91 |

476 6. Conclusions

477 In many recognition and classification problems, the most time and resource consuming part is
 478 the feature extraction process. Many scientists focus on extracting meaningful features from the EEG
 479 signals either in time and/or frequency domain in order to achieve successful classification results.
 480 However, the derived feature sets, which can be useful in the classification problem for one subject,
 481 recording session or dataset can fail for different subjects, recording sessions and datasets.
 482 Furthermore, since the feature extraction process is a complex and time-consuming process, it is not
 483 particularly suitable for online and real time classification problems. In this study, we do not rely on
 484 a separate pre-feature extraction process and shift this task to the deep learning cycle that inherently
 485 employs this process. Hence, we do not manually remove any potentially useful information from
 486 the raw EEG channels. Similar approaches, where deep neural networks are utilized for recognition,
 487 were applied in different domains, such as in [86] where electromagnetic sources can be recognised.
 488 The success of CNNs has already been shown as highly competent in various classification tasks,
 489 especially in the image classification context. Therefore, we deploy of a pretrained CNN architecture
 490 called InceptionResnetV2 to classify the EEG data. We have taken the necessary steps to reshape the
 491 input data to feed into and train this network.

492 One of the most important issues, which influences the success of deep learning approaches is
 493 the data itself and the quality and reliability of the labels of the data. The “Brouwer
 494 recommendations” about data collection given in [19] are very useful for handling accurate data and
 495 labelling. Especially during the EEG data recording process, these recommendations should be
 496 double checked due to the EEG recording device’s sensitivity to noise.

497 EEG signals are non-stationary and nonlinear. This makes putting forth a general classification
 498 model and a set of features based on the well-studied spectral band powers difficult. It is important
 499 to be able to identify stable feature sets between subjects, recording sessions and datasets. Since for

500 complex classification problems, CNN is very successful in extracting not-so-obvious features from
501 the input data, we exploit a state of the art pretrained CNN model called InceptionResnetV2 and do
502 not filter out any information from the raw EEG signals. For robustness, we further enrich this deep
503 network by adding fully connected dense layers. This increases the depth and prevents the network
504 from falling into probable ill-conditions and overfitting problems.

505 In this work, we applied the model successfully on three different EEG datasets: SEED, DEAP
506 and LUMED. Furthermore, we tested our model in a cross-dataset context. We have trained our
507 model with SEED dataset, tested on DEAP and LUMED dataset. Moreover, we have trained our
508 model with DEAP dataset and tested on LUMED dataset. We showed that the results are promising
509 and superior to most of the reference techniques. Once we generate the fully pre-trained model, we
510 can feed any online raw data directly as input to get the output class immediately. Since there is not
511 a dedicated pre-feature extraction process, our model is more suitable to be deployed in real-time
512 applications.
513

514 **Author Contributions:** Conceptualization, Y.C.; methodology, Y.C.; software, Y.C.; validation, Y.C.; formal
515 analysis, Y.C.,E.E.; investigation, Y.C.; resources, Y.C.; data curation, Y.C.; writing—original draft preparation,
516 Y.C.,E.E.; writing—review and editing, Y.C., E.E.; visualization, Y.C.,E.E.; supervision, E.E.; project
517 administration, Y.C., E.E; funding acquisition, E.E.

518 **Funding:** This work was supported by an Institutional Links grant, ID 352175665, under the Newton - Katip
519 Celebi partnership between the UK and Turkey. The grant is funded by the UK Department of Business, Energy
520 and Industrial Strategy (BEIS) and The Scientific and Technological Research Council of Turkey (TUBITAK) and
521 delivered by the British Council. For further information, please visit www.newtonfund.ac.uk.

522 **Acknowledgments:** We would like to thank the creators of DEAP and SEED datasets for openly sharing them
523 with us and the wider research community. The authors would also like to thank all volunteering staff and
524 students in Loughborough University London for participating in the recording sessions to generate the LUMED
525 dataset.

526 **Conflicts of Interest:** The authors declare no conflict of interest.

527 References

- 528 1. Top 14 EEG Hardware Companies: Available online: [https://imotions.com/blog/top-14-eeeg-hardware-](https://imotions.com/blog/top-14-eeeg-hardware-companies-ranked/)
529 [companies-ranked/](https://imotions.com/blog/top-14-eeeg-hardware-companies-ranked/) (accessed on 09/02/2020).
- 530 2. Valer J., Daisuke T., Ippeita D., 10/20, 10/10, and 10/5 systems revisited: Their validity as relative head-
531 surface-based positioning systems, *Journal of NeuroImage*, **2007**, Volume 34, Issue 4, Pages 1600-1611, ISSN
532 1053 8119, <https://doi.org/10.1016/j.neuroimage.2006.09.024>.
- 533 3. Aboalayon K.A.I., Faezipour M., Almuhammadi W.S., and Moslehpour S., Sleep stage classification using EEG
534 signal analysis: a comprehensive survey and new investigation, *MDPI Journal of Entropy*, **2016**, Vol. **18** 272.
- 535 4. Acharya U.R., Sree S. V., Swapna G., Martis R. J., and Suri J.S., Automated EEG analysis of epilepsy: a review,
536 *Journal of Knowledge-Based Systems*, **2013**, Vol. 45, Pages.147–65.
- 537 5. Engemann D.A. et al, Robust EEG-based cross-site and cross-protocol classification of states of consciousness,
538 *Journal of Brain*, **2018**, Vol. 141, Pages 3179–92.
- 539 6. Arns M., Conners C. K., and Kraemer H. C., A decade of EEG theta/beta ratio research in ADHD: a meta-analysis,
540 *Journal of Attention Disorders*, **2013**, Vol. 17, Pages 374–83.
- 541 7. Liu N.H., Chiang C.Y., Chu H.C., Recognizing the degree of human attention using EEG signals from
542 mobile sensors, *Journal of Sensors (Basel)*. **2013**, Vol. 13(8), Pages. 10273–10286, doi:10.3390/s130810273
- 543 8. Shestyuk A.Y., Kasinathan K., Karapoondinott V., Knight R.T., Gurumoorthy R., Individual EEG measures
544 of attention, memory, and motivation predict population level TV viewership and Twitter
545 engagement. *Journal of PLOS One*, **2019**, Vol. 14(3), doi:10.1371/journal.pone.0214507.
- 546 9. Mohammadpour M., and Mozaffari S., Classification of EEG-based attention for brain computer interface,
547 *3rd Iranian Conference on Intelligent Systems and Signal Processing (ICSPIS), Shahrood*, **2017**, Pages 34-37. doi:
548 10.1109/ICSPIS.2017.8311585.
- 549 10. So W.K.Y., Wong S.W.H., Mak J.N., Chan R.H.M., An evaluation of mental workload with frontal EEG.
550 *Journal of PLOS ONE*, **2017**, Vol. 12(4), <https://doi.org/10.1371/journal.pone.0174949>.

- 551 11. Thejaswini S., Ravikumar K.M., Jhenkar L., Aditya N., Abhay K.K., Analysis of EEG Based Emotion
552 Detection of DEAP and SEED-IV Databases using SVM, *International Journal of Recent Technology and*
553 *Engineering (IJRTE)*, **2019**, Vol. 8, Issue-1C, Pages 207-211, ISSN: 2277-3878.
- 554 12. Liu J., Meng H., Nandi A., and Li M., Emotion detection from EEG recordings, *12th International Conference*
555 *on Natural Computation, Fuzzy Systems and Knowledge Discovery (ICNC-FSKD)*, **2016**, Changsha, Pages 1722-
556 1727.
- 557 13. Gómez A., Quintero L., López N., Castro J., An approach to emotion recognition in single-channel EEG
558 signals: a mother child interaction, *Journal of Physics: Conference Series*, **2016**, Vol. 705.
- 559 14. Xing X., Zhenqi L., Tianyuan X., Shu L., Hu B., and Xiangmin X., SAE+LSTM: A New Framework for
560 Emotion Recognition From Multi-Channel EEG, *Journal of Frontiers in Neurobotics*, **2019**, Volume 13.
561 <https://doi.org/10.3389/fnbot.2019.00037>.
- 562 15. Müller-Putz G., Peicha L., Ofner P., Movement Decoding from EEG: Target or Direction, *Graz Brain-*
563 *Computer Interface Conference*, **2017**, doi: 10.3217/978-3-85125-533-1-63.
- 564 16. Padfield N., Zabalza J., Zhao H., Masero V., Ren J., EEG-Based Brain-Computer Interfaces Using Motor-
565 Imagery: Techniques and Challenges. *MDPI Journal of Sensors*, **2019**, Vol. 19(6), 1423. doi:10.3390/s19061423.
- 566 17. Haufe S., Mondini A.U., Valeria M., Anna L., Cappello A., EEG-Based BCI System Using Adaptive Features
567 Extraction and Classification Procedures, *Journal of Computational Intelligence and Neuroscience*, **2016**,
568 <https://doi.org/10.1155/2016/4562601>.
- 569 18. Picard R.W., Affective Computing, MIT Media Laboratory, *Perceptual Computing*; **1995**, 20 Ames St.,
570 Cambridge, MA 02139.
- 571 19. Alarcão S.M., and Fonseca M. J., Emotions Recognition Using EEG Signals: A Survey, *IEEE Transactions on*
572 *Affective Computing*, **2019**, Vol. 10, no. 3, Pages 374-393, doi: 10.1109/TAFFC.2017.2714671.
- 573 20. Ekman P., Friesen W.V., O'Sullivan M., Chan A.I., Diacoyanni T., Heider K., Krause R., LeCompte W.A.,
574 Pitcairn T., and Ricci-Bitti P. E., Universals and cultural differences in the judgments of facial expressions
575 of emotion. *Journal of Personality and Social Psychology*, **1987**, vol. 53, no. 4, Pages 712–717, doi: 10.1037/0022-
576 3514.53.4.712.
- 577 21. Scherer K.R., What are emotions? And how can they be measured, *SAGE Journals: Social Science Information*,
578 **2005**, Vol. 44, no. 4, Pages 695-729, <https://doi.org/10.1177/0539018405058216>.
- 579 22. Koelstra S., Mueh C., Soleymani M., Lee J.-S., Yazdani A., Ebrahimi T., Pun T., Nijholt A., Patras I., DEAP:
580 A Database for Emotion Analysis using Physiological Signals, *IEEE Transactions on Affective Computing*,
581 **2011**, Vol. 3, no. 1, Pages 18-31.
- 582 23. Russell J. A., A circumplex model of affect, *Journal of Personality and Social Psychology*, **1980**, Vol. 39, no. 6,
583 Pages. 1161–1178.
- 584 24. Guzel Aydin S., Kaya T., Guler H., Wavelet-based study of valence-arousal model of emotions on EEG
585 signals with LabVIEW, *Journal of Brain Informatics*, **2016**, Vol. 3(2), Pages 109–117, doi:10.1007/s40708-016-
586 0031-9.
- 587 25. Paltoglou G., and Thelwall M., Seeing Stars of Valence and Arousal in Blog Posts, *IEEE Transactions on*
588 *Affective Computing*, **2013**, Vol. 4, no. 1, Pages 116-123, doi: 10.1109/T-AFFC.2012.36.
- 589 26. The McGill Physiology Virtual Lab: Available online:
590 https://www.medicine.mcgill.ca/physio/vlab/biomed_signals/eeg_n.htm (09/02/2020).
- 591 27. Al-Fahoum A.S., Al-Fraihat A., Methods of EEG Signal Features Extraction Using Linear Analysis in
592 Frequency and Time-Frequency Domains, *ISRN neuroscience*, **2014**, doi:10.1155/2014/730218.
- 593 28. Ruo-Nan D., Jia-Yi Z., and Bao-Liang L., Differential Entropy Feature for EEG-based Emotion
594 Classification, *6th International IEEE/EMBS Conference on Neural Engineering (NER)*, **2013**, San Diego, CA,
595 Pages 81-84.
- 596 29. Wei-Long Z., and Bao-Liang L., Investigating Critical Frequency Bands and Channels for EEG-based
597 Emotion Recognition with Deep Neural Networks, **2015**, *IEEE Transactions on Autonomous Mental*
598 *Development (IEEE TAMD)*, Vol. 7(3), Pages 162-175.
- 599 30. George F.P., Shaikat I.M., Hossain P.S.F., Parvez M.Z., Uddin J., Recognition of emotional states using EEG
600 signals based on time-frequency analysis and SVM classifier, *International Journal of Electrical and Computer*
601 *Engineering (IJECE)*, **2019**, Vol. 9, Pages 1012-1020.
- 602 31. Soundarya S., An EEG based emotion recognition and classification using machine learning techniques,
603 *International Journal of Emerging Technology and Innovative Engineering*, **2019**, Volume 5, Issue 4, Pages 744-
604 750.

- 605 32. Swati V., Preeti S., Chamandeep K., Classification of Human Emotions using Multiwavelet Transform
606 based Features and Random Forest Technique, *Indian Journal of Science and Technology*, **2015**, Vol 8.
- 607 33. Bono V., Biswas D., Das S., and Maharatna K., Classifying human emotional states using wireless EEG
608 based ERP and functional connectivity measures, *IEEE-EMBS International Conference on Biomedical and*
609 *Health Informatics (BHI)*, **2016**, Las Vegas, NV, 2016, pp. 200-203. doi: 10.1109/BHI.2016.7455869.
- 610 34. Nattapong T., Ken-ichi F., Masayuki N., Application of Deep Belief Networks in EEG, based Dynamic
611 Music-emotion Recognition, *The International Joint Conference on Neural Networks (IJCNN)*, **2016**, Vancouver,
612 Canada.
- 613 35. Prieto L., and Kominkova O., Emotion Recognition using AutoEncoders and Convolutional Neural
614 Networks. *MENDEL*. **2018**, vol. 24, no. 1, Pages 113-120, doi: 10.13164/mendel.2018.1.113
- 615 36. Chen J. X., Zhang P. W., Mao Z. J., Huang Y. F., Jiang D. M., and Zhang Y. N., Accurate EEG-Based Emotion
616 Recognition on Combined Features Using Deep Convolutional Neural Networks, **2019**, *IEEE Access*, Vol. 7,
617 Pages 44317-44328.
- 618 37. Tripathi S., Acharya S., Sharma R. D., Mittal S., and Bhattacharya S., Using deep and convolutional neural
619 networks for accurate emotion classification on DEAP Dataset, *Proceedings of the Thirty-First AAAI*
620 *Conference on Artificial Intelligence*, **2017**, Pages 4746-4752.
- 621 38. Salama E. S., El-Khoribi R. A., Shoman M. E., and Shalaby M. A., EEG-based emotion recognition using 3D
622 convolutional neural networks, *International Journal of Advanced Computer Science and Applications(IJACSA)*,
623 **2018**, vol. 9, no. 8, Pages 329-337.
- 624 39. Alhagry S., Aly A., El-Khoribi R., Emotion Recognition based on EEG using LSTM Recurrent Neural
625 Network, *International Journal of Advanced Computer Science and Applications*, **2017**, Vol. 8, Pages 355-358.
- 626 40. Jeevan R. K., Shiva Kumar P., Srivikas M., EEG-based emotion recognition using LSTM-RNN machine
627 learning algorithm, *1st International Conference on Innovations in Information and Communication Technology*
628 *(ICIICT)*, **2019**, Pages 1-4.
- 629 41. Li M., Xu H., Liu X., Lu S. Emotion recognition from multichannel EEG signals using K-nearest neighbor
630 classification. *Journal of Technology and Health Care*, **2018**, Vol. 26, Pages 509–519, doi:10.3233/THC-174836.
- 631 42. Alazrai R., Homoud R., Alwanni H., Daoud M.I., EEG-Based Emotion Recognition Using Quadratic Time-
632 Frequency Distribution. *MDPI Sensors*, **2018**, Vol. 18, No. 8, 2739, doi:10.3390/s18082739
- 633 43. Nivedha R., Brinda M., Vasanth D., Anvitha M., and Suma K. V., EEG based emotion recognition using
634 SVM and PSO, *International Conference on Intelligent Computing, Instrumentation and Control Technologies*
635 *(ICICT)*, **2017**, Kannur, Pages 1597-1600.
- 636 44. Pan S.J., et. al., Domain adaptation via transfer component analysis. *IEEE Transaction on Neural Network*,
637 **2011**, Vol. 22, No. 2, Pages 199–210.
- 638 45. Chai X., et. al.: Unsupervised domain adaptation techniques based on auto-encoder for non-stationary
639 EEG-based emotion recognition. *Journal of Computers in Biology and Medicine*, **2016**, Vol. 79, Pages 205–214.
- 640 46. Weiwei Z., Cross-Subject EEG-Based Emotion Recognition with Deep Domain Confusion, *Intelligent*
641 *Robotics and Applications. ICIRA 2019. Lecture Notes in Computer Science*, **2019**, Vol. 11740.
- 642 47. Pallavi P., Seeja K.R., Subject independent emotion recognition from EEG using VMD and deep learning,
643 *Journal of King Saud University - Computer and Information Sciences*, **2019**, Pages 53-58
- 644 48. Fu Y., Xingcong Z., Wenge J., Pengfei G., Guangyuan L., Multi-method Fusion of Cross-Subject Emotion
645 Recognition Based on High-Dimensional EEG Features, *Frontiers in Computational Neuroscience*, **2019**,
646 Volume 13.
- 647 49. Keelawat P., Thammasan N., Kijirikul B., Numao M., Subject-Independent Emotion Recognition During
648 Music Listening Based on EEG Using Deep Convolutional Neural Networks, *IEEE 15th International*
649 *Colloquium on Signal Processing & Its Applications (CSPA)*, **2019**, Penang, Malaysia, Pages 21-26.
650 10.1109/CSPA.2019.8696054.
- 651 50. Yang F., Zhao X., Jiang W., Gao P., Liu G., Multi-method Fusion of Cross-Subject Emotion Recognition
652 Based on High-Dimensional EEG Features, *Frontiers in Computational Neuroscience*, **2019**,
653 doi:10.3389/fncom.2019.00053.
- 654 51. Gupta V., Chopda M. D., Pachori R. B., Cross-Subject Emotion Recognition Using Flexible Analytic Wavelet
655 Transform From EEG Signals, in *IEEE Sensors Journal*, **2019**, Vol. 19, no. 6, Pages 2266-2274.
- 656 52. Zhong Y., Yongxiong W., Li L., Wei Z., Jianhua Z., Cross-Subject EEG Feature Selection for Emotion
657 Recognition Using Transfer Recursive Feature Elimination, *Frontiers in Neurorobotics*, **2017**, Vol. 11.

- 658 53. Zhong P., Wang D., Miao C., EEG-Based Emotion Recognition Using Regularized Graph Neural Networks,
659 arXiv.org, in Press, **2019**.
- 660 54. Pan S. J. and Yang Q., A survey on transfer learning, *IEEE Transaction on Data Engineering*, **2010**, Vol. 22,
661 no. 10, Pages 1345–1359.
- 662 55. Krauledat M., Tangermann M., Blankertz B., and Müller K. R., Towards zero training for brain-computer
663 interfacing, *Journal of PLOS ONE*, **2008**, Vol. 3, no. 8.
- 664 56. Fazli S., et. al., Subject-independent mental state classification in single trials, *Journal of Neural Networks*,
665 **2009**, Vol. 22, no. 9, Pages. 1305–1312.
- 666 57. Kang H., Nam Y., and Choi S., Composite common spatial pattern for subject-to-subject transfer, *IEEE*
667 *Signal Processing Letters*, **2009**, Vol. 16, no. 8, Pages 683–686.
- 668 58. Zheng W.L., Zhang Y.Q., Zhu J.Y., and Lu B.L., Transfer components between subjects for EEG-based
669 emotion recognition, *2015 International Conference on Affective Computing and Intelligent Interaction (ACII)*,
670 **2015**, Xi'an, China, Pages 917–922.
- 671 59. Zheng W.-L., and Lu B.-L., Personalizing EEG-based affective models with transfer learning, *Proceedings of*
672 *the Twenty-Fifth International Joint Conference on Artificial Intelligence (IJCAI-16)*, **2016**, Pages 2732–2738.
- 673 60. Chai X., et al., Unsupervised domain adaptation techniques based on auto-encoder for non-stationary EEG-
674 based emotion recognition, *Journal of Computers in Biology and Medicine*, **2016**, Vol. 79, Pages 205–214.
- 675 61. Chai X., et al., A fast, efficient domain adaptation technique for cross-domain electroencephalography
676 (EEG)-based emotion recognition, *MDPI Sensors*, **2017**, Vol. 17, no. 5, Page 1014.
- 677 62. Zirui L., Sourina O., Wang L., Scherer R., Müller-Putz G., Domain Adaptation Techniques for EEG-Based
678 Emotion Recognition: A Comparative Study on Two Public Datasets, *IEEE Transactions on Cognitive and*
679 *Developmental Systems*, **2018**, Vol.11, Pages 85-94, 10.1109/TCDS.2018.2826840.
- 680 63. Chai X., et. al., Efficient Domain Adaptation Technique for Cross-Domain Electroencephalography (EEG)-
681 Based Emotion Recognition, *MDPI Sensors*, **2017**, Vol.17, Page 1014.
- 682 64. Tzeng E., et. al., Deep domain confusion: maximizing for domain invariance, *arXiv preprint arXiv:1412.3474*,
683 **2014**.
- 684 65. SEED Dataset. Available online: <http://bcmi.sjtu.edu.cn/~seed/> (accessed on 09/02/2020).
- 685 66. DEAP Dataset. Available online: <https://www.eecs.qmul.ac.uk/mmv/datasets/deap/> (accessed on
686 09/02/2020).
- 687 67. Pretrained Deep Neural Networks, Available online:
688 <https://uk.mathworks.com/help/deeplearning/ug/pretrained-convolutional-neural-networks.html>
689 (accessed on 09/02/2020).
- 690 68. Keras Applications. Available online: <https://keras.io/applications/#inceptionresnetv2> (accessed on
691 09/02/2020).
- 692 69. Lane A., Beedie C., Terry P., Distinctions between Emotion and Mood. *Journal of Cognition and Emotion*.
693 **2005**, Vol. 19, doi: 10.1080/02699930541000057.
- 694 70. Particle Swarm Optimization, Available online:
695 <https://www.sciencedirect.com/topics/engineering/particle-swarm-optimization> (accessed on 09/02/2020)
- 696 71. SEED Dataset. Available online: <http://bcmi.sjtu.edu.cn/~seed/seed-iv.html> (accessed on 09/02/2020).
- 697 72. Salzman C. D., Fusi S., Emotion, cognition, and mental state representation in amygdala and prefrontal
698 cortex, *Journal of Annual Review of Neuroscience*, **2010**, Vol. 33, Pages 173-202, doi:
699 10.1146/annurev.neuro.051508.135256.
- 700 73. Zhao G., Zhang Y., Ge Y., Frontal EEG Asymmetry and Middle Line Power Difference in Discrete Emotions,
701 *Frontiers in Behavioral Neuroscience*, **2018**, Vol.12, Page 225.
- 702 74. Bos P. -O. D., EEG-based Emotion Recognition. The Influence of Visual and Auditory Stimuli, **2006**.
- 703 75. Al-Nafjan A., Al-Wabil A., Hosny M., Al-Ohali Y., Classification of Human Emotions from
704 Electroencephalogram (EEG) Signal using Deep Neural Network, *(IJACSA) International Journal of Advanced*
705 *Computer Science and Applications*, **2017**, Vol. 8, No. 9.
- 706 76. Loughborough University EEG based Emotion Recognition Dataset. Available online:
707 https://www.dropbox.com/s/xlh2orv6mgweehq/LUMED_EEG.zip?dl=0
- 708 77. Gong B., Shi Y., Sha F., and Grauman K., Geodesic flow kernel for unsupervised domain adaptation
709 *Proceedings of the IEEE Conference on Computer Vision and Pattern Recognition(CVPR)*, **2012**, Pages 2066-
710 2073.

- 711 78. Schölkopf B., Smola B., and Müller K. R., Nonlinear component analysis as a kernel eigenvalue problem,
712 *Neural computation*, **1998**, Vol. 10, no. 5, Pages 1299-1319.
- 713 79. Yan K., Kou L., and Zhang D., Learning Domain-Invariant Subspace Using Domain Features and
714 Independence Maximization, *IEEE Transactions on Cybernetics*, **2018**, vol. 48, no. 1, Pages. 288-299.
- 715 80. Fernando B., Habrard A., Sebban M., and Tuytelaars T., Unsupervised visual domain adaptation using
716 subspace alignment, *Proceedings of the IEEE International Conference on Computer Vision*, **2013**, Pages 2960-
717 2967.
- 718 81. Shi Y., and Sha F., Information-theoretical learning of discriminative clusters for unsupervised domain
719 adaptation, *Proceedings of the International Conference on Machine Learning (ICML)*, **2012**, Pages 1275–1282.
- 720 82. Enobio 8. Available online: <https://www.neuroelectrics.com/solutions/enobio/8/> (accessed on 09/02/2020).
- 721 83. Wang F., Zhong S., Peng J., Jiang J., Liu Y., Data Augmentation for EEG-Based Emotion Recognition with
722 Deep Convolutional Neural Networks, In: Schoeffmann K. et al. (eds) *MultiMedia Modeling. MMM. Lecture*
723 *Notes in Computer Science*, **2018**, Vol. 10705. Springer, Cham.
- 724 84. Kawala-Sterniuk A., et. al., Comparison of Smoothing Filters in Analysis of EEG Data for the Medical
725 Diagnostics Purposes, **2020**, *MDPI Sensors*, Vol. 20, No. 3, Page 807, doi: 10.3390/s20030807
- 726 85. Tang C., et. al., EEG-based emotion recognition via fast and robust feature smoothing, **2017**, *Proceedings of*
727 *International Conference on Brain Informatics*, Pages 83-92.
- 728 86. Matuszevski J., and Pietrow D., Recognition of electromagnetic sources with the use of deep neural
729 networks, *Proc. SPIE 11055, XII Conference on Reconnaissance and Electronic Warfare Systems*, **2019**,
730 <https://doi.org/10.1117/12.2524536>.
- 731 87. Plöchl M., Ossandón J.P., König P., Combining EEG and eye tracking: identification, characterization, and
732 correction of eye movement artifacts in electroencephalographic data. *Front Hum Neuroscience*, **2012**, Vol.
733 6:278. doi:10.3389/fnhum.2012.00278.



© 2020 by the authors. Submitted for possible open access publication under the terms and conditions of the Creative Commons Attribution (CC BY) license (<http://creativecommons.org/licenses/by/4.0/>).